Emergency Landing Decision Method for Unmanned Aircraft

Gomez, Aitor Ramirez; la Cour-Harbo, Anders

Published in:
2021 International Conference on Unmanned Aircraft Systems (ICUAS)

DOI (link to publication from Publisher):
10.1109/ICUAS51884.2021.9476792

Publication date:
2021

Document Version
Accepted author manuscript, peer reviewed version

Emergency Landing Decision Method for Unmanned Aircraft

Aitor Ramirez Gomez* and Anders la Cour-Harbo

Abstract— **This paper describes a framework to generate a computationally low-cost decision function to automate emergency landings for drones. Specifically, this function makes a choice of which is the most suitable location to land an unmanned aircraft from a given list of candidate ground locations. The candidate ground locations are described by a distance metric from the aircraft to the landing location and by a probability safety measure associated to how safe it is to land in that particular location. In addition, an urgency level, associated with the current healthy status of the unmanned aircraft, and a tuning parameter that models its robustness are included in the decision function. These four parameters are assumed to be given and to have some particular properties, which are described further in the paper.**

I. INTRODUCTION

The unmanned aircraft systems (UAS) usage for industry and military operations have become more appealing within the past years. Commercial and health-care applications that are subjected to fly across urban areas, such as package or medical product delivery, are also showing their interest [1], [2]. However, the accident rate of UAS is still significantly higher than the equivalent rate for manned aircraft, with the former being around 1 per 1000 hours of flight [3]. In the same direction, students proved using failure mode effect and analysis (FMEA) having an average of 2.17 failures leading to flight termination per 100 flight hours of an Ultra Stick 120 [5]. These numbers are rather high for UAS to achieve functional status and full social acceptance, and hence, a clear way to reduce the concern is by incorporating contingency strategies to the system to mitigate the risks of undesired hazardous events that could also lead to third-party damage, injuries, or even casualties. These undesired events could be modeled by probability distributions that would be used to design a contingency plan, but the amount of flight hours required in the same specific conditions prevents this task from being affordable in any sense [6]. This is the main motivation for the context of this work. In the research project SafeEYE [7], we have previously proposed a framework able to mitigate the risk of UAS operations and prevent escalation, namely, an automated emergency landing system. This type of system requires various subsystems to cope with the outcome of such demanding task, and this paper focuses on one of these subsystems. Some of these subsystems are related to self-awareness of the drone, by introducing sensors and developing algorithms able to understand the safety status of the drone and/or its remaining life-time. Other subsystems are related to the environment sensing, which gives insight on the surroundings of the aircraft and how to navigate. The work presented here focus on one particular task of the latter, i.e. decision-making. An efficient low-complexity algorithm is then proposed, which incorporates three essential safety features related to the emergency landing problem:

1) Urgency to perform landing, being an emergency level associated to remaining flight time of the drone.
2) Metric describing distance/time to travel from the current position to a potential landing locations.
3) Probabilistic measure associated to the risk of landing on the potential locations.

In addition, a fourth parameter that models the robustness of the particular aircraft is introduced in the decision problem to allow the user some flexibility. This parameter is assumed completely tune-able, and providing guidelines on how to determine a specific value of this parameter for a given aircraft is out of the scope of this paper.

A. Background

The work presented here is part of the SafeEYE project, which implements an automated system for safe emergency landing. SafeEYE is divided into three conceptually different steps, which are

1) Detection of malfunction **(Detect)**
2) Recognizing landing spots **(Find)**
3) Planning and guidance for landing **(Land)**

A more detailed description of the SafeEYE project is provided in [7], where the manner in which the different steps are interconnected and dependent on each other is described. The focus of this paper is on the third step *Land*, which is highly dependent on the two previous steps. The basic objective of *Detect* is to quantify the urgency of landing at any given instant during flight by detecting potential component malfunctions. The basic objective of *Find* is to visually identify and store possible ground landing locations and their probability measure (safety to land) by classifying ground images from an on-board camera. The basic objective of *Land* is to determine the best place to attempt landing, given the information from the two previous steps, and to design a scheme of consecutive actions to autonomously guide a faulty aircraft to the best ground landing location, in the safest way possible according to a criteria based on these three parameters. In some severe situations, these actions should accommodate the possibility of guiding the drone to a certain location in order to perform a crash landing. Such task is achieved by answering two basic questions: "where to land" and "how to land". In this paper, we present the design of a tool that gives answer to the first question: where to land.

Automation and Control, Department of Electronic Systems, Aalborg University, Fredrik Bajers Vej 7C 9220 Aalborg Denmark
arg@es.aau.dk, alc@es.aau.dk

B. Related Work

Different criteria are used in the literature to select the most appropriate decision among a discrete set of options. Despite some of them being designed for purposes other than emergency landings, ideas can still be borrowed. In [4], [8], stereo cameras are used to map and classify the terrain as safe according to height, roughness, slope, land-able space and other parameters, and then optimizing the distance with respect to certain points of interest to select the final landing site. Other optimal approaches include [9], in which terrain, fuel consumption and performance are incorporated in the optimization problem to select the landing site in a planetary landing mission. In [10], a weighted sum with different normalized measures that contribute to safety is employed to generate scores that are eventually used to rank the landing sites. Similarly, in [13] a weighted sum is utilized to select at every instant the best action to be executed by a self-driving car. Machine learning methods are also extensively used in the literature for ground image classification. However, the landing site selection is still not linked to the classification problem, but rather set as a posterior problem to solve. For instance, in [12] the K-nearest neighbor method is employed to classify ground images as *clear*, *partially clear*, and *unclear* in three different lightning conditions to perform safe landing. The selection of the final landing locations is basically made by taking the next image classified as *clear*, if time is not critical. When time is critical, the algorithm goes through the last n images processed looking for a *clear* or *partially clear* classification, and if an empty set is returned it keeps analyzing new ground images until one is finally found.

C. Contribution

The major contribution presented in this work is a framework to generate a low-complexity function that can be combined with three essential safety-related independent parameters in order to determine in real-time where to attempt an emergency landing procedure. That is, a function able to take the decision by accommodating: the current urgency level of landing, and the pair distance and probability measure of the classified landing locations. By combining these parameters, a decision function is proposed in Section II to select the most suitable ground location to land from the set of detected locations. The function also accommodates a tuning parameter that allow the user to act directly in the decision process for a more refined tuning. The process of verifying the proposed decision function in an automated manner in order to earn statistical significance of the results is complex due to restricting ourselves from working with data models, but also due to the lack of one such database. Subsequently, a brief analysis of the proposed function is performed in Section III supported by simulations conducted to prove the performance of the solution under several randomized scenarios. Experimental tests meant to show the effectiveness of the solution under real scenarios are left as future work, after completion of the SafeEYE project and once all the functionalities (*Detect*, *Find* and *Land*) are operating together.

II. METHOD

The landing location selector is a mathematical function that takes three arguments, and produces a single *cost* value. The arguments taken are related to one landing location, and the cost function quantifies how risky is to perform landing in this specific landing location. Notation is introduced to facilitate the formulation of the problem mathematically.

1) $\mu \geq 0$ is the current urgency level,
2) $R_p > 0$ is the distance from aircraft to landing location p, and
3) $\lambda_p \in [0, 1]$ is the probability measure showing the confidence level that location p is a safe landing site.

The cost for a specific location p is named J_p, and $\mathbf{R}$ is a vector of all R_p values.

In our use, R is the Euclidean distance between the aircraft and the landing location, but the formulation of the problem allows for R to be another measure, such as the total trajectory distance travelled, or the total time needed to reach the landing location. Since λ_p and R_p are, in any case, independent, their contributions to the cost J_p are introduced separately. However, in order to generate the cost function, the parameter R_p has been normalized using the one-norm $\|\cdot\|_1$ as

$$\bar{R}_p = \frac{R_p}{\|\mathbf{R}\|_1} , \tag{1}$$

so that its contribution to J_p is comparable to λ_p. To perform (1) two assumptions have to be considered: 1) the vector $\mathbf{R}$ is never empty, meaning that at least one location has been detected and stored, and 2) R_p is never zero when there is only one location stored. With this, the parameters λ_p and $\bar{R}_p$ are now equally bounded and can be utilized to generate the cost function. Eventually, J_p will form a changing multi-criteria cost function that takes the contribution of λ_p and $\bar{R}_p$ to the cost for a given urgency level, namely the contribution of these two location parameters can vary depending on μ. In this project only μ, λ_p and $\bar{R}_p$ are tackled to assess a first iteration of the problem, but clearly this can be upgraded by adding the contribution of other parameters, e.g. the velocity of the drone, wind, clusters of landing locations, etc., to the cost function, which also add extra degrees of complexity to solve the problem.

A. Decision Function

Taking μ, λ_p, and $\bar{R}_p$, the function $J_p : \mathbb{R}^3 \to \mathbb{R}$ has been expressed as an elliptic paraboloid, meaning that the level curves of J_p are ellipses, and the principal axes of the level curves are aligned with the parameters λ_p and $\bar{R}_p$. This choice was made due to the well-known quadratic properties, making it easy to model in order to fit the requirements. Furthermore, the shape of the paraboloid, or more specifically the magnitude of the principal axes of the level curves, also change by effect of the urgency level μ.

Such a function, able to quantify the suitability of the landing spot according to this, is shown below.

$$J_p(\mu, \lambda_p, \bar{R}_p) = w_1(\mu)\alpha\frac{\left(1-\lambda_p\right)^2}{a} + w_2(\mu)(1-\alpha)\frac{\bar{R}_p^2}{b} \quad (2)$$

Note that a sufficiently good landing site p is defined by a big enough value of λ_p and a small enough value of $\bar{R}_p$. In order to be coherent with the direction of optimization, the penalization is instead applied to the *uncertainty* measure of the landing site defined as $(1-\lambda_p)$ as it can be seen in (2), rather than the confidence measure itself. With this, it is sought for a small enough value of both terms, which leads to an overall small value of the general cost J_p. Henceforth, for a general set $\mathbf{\Lambda}$ of P landing spots, $\mathbf{\Lambda} = \left\{(\lambda_1, \bar{R}_1), (\lambda_2, \bar{R}_2), ..., (\lambda_P, \bar{R}_P)\right\}$, the most suitable landing spot is the element whose cost J_p is minimal. This is mathematically expressed as

$$\min_{(\lambda_p, \bar{R}_p)\in\mathbf{\Lambda}} J_p(\mu, \lambda_p, \bar{R}_p)\ . \quad (3)$$

Then, it can be deduced that the terms $(1-\lambda_p)$ and $\bar{R}_p$ in (2) are the penalizations applied to the probability measure and the distance of the location p, respectively, and $w_1(\mu)$ and $w_2(\mu)$ are weights applied to each of the penalizations whose values change with μ. Parameter μ is changing according to the urgency level of the current status of the aircraft in a monotone way, either linearly or in any non-linearly, and depends on the malfunctions and the method employed to determine μ. The assumptions is that increase of the urgency value means that the remaining time to perform a safety landing is shortened. This increase in μ, then, demands a similar change in the penalizations of λ and $\bar{R}$, which has been modeled as

$$w_1(\mu) = e^{-\mu}, \text{ and}$$
$$w_2(\mu) = e^{\mu}\ .$$

This means that the importance of closer locations will be more relevant than higher values of λ, for increasing urgency values. The parameter $\alpha \in [0, 1]$ can be found in both terms of (2), and has the function of being a tune-able parameter for the user given the variability of the possible aircraft using the algorithm. It allows the user to alter the balance of the contribution of λ and $\bar{R}$ in the cost function, providing the opportunity for selecting landing locations further away if the aircraft is thought to be robust enough, or the other way around otherwise. In order to standardize the work presented in this paper, it has been deemed convenient to proceed with $\alpha = 0.5$. It is the responsibility of the user to adjust this parameter for a more refined tuning, suited for the specifications of the aircraft at hand.

The parameters a and b in (2) are the paraboloid parameters used to shape the function J_p. In order to find proper a and b values, two things are considered.

1) a constraint in the parameters a and b, and
2) multiple pair points $(\mu, \lambda_p, \bar{R}_p)$ that are assumed to provide similar cost values.

i	**1**	**2**	**3**	**4**	**5**
$\boldsymbol{\mu_i}$	0	0	0.5	1	2
$\boldsymbol{\lambda_{i,1}}$	0.4	0.93	0.8	0.6	0.3
$\mathbf{\bar{R}_{i,1}}$	0.2	0.9	0.1	0.8	0.8
$\boldsymbol{\lambda_{i,2}}$	0.4	0.97	0.9	0.65	0.35
$\mathbf{\bar{R}_{i,2}}$	0.05	0.9	0.2	0.8	0.8

TABLE I: Containing $N = 5$ pairs of $(\mu, \lambda_p, \bar{R}_p)$ points that are considered to have roughly the same cost value. The pairs can be read column-wise, each of the points in the same pair (column) sharing the parameter μ.

These points are chosen out of the intuition of the authors provided by their experience in the field, and thus present no analytical dissemination.

The constraint on the parameters a and b is meant to achieve balance between the axes of the paraboloid, as well as to simplify the optimization problem. Such constraint will be of the form $a+b = C$, Where $C \in \mathbb{R}_+$ is a strictly positive constant, since negative values of C would solve for negative values of a and b, turning the cost function upside down, and for $C = 0$ the solution becomes trivial ($a = b = 0$). Despite the solution for a and b also changing with positive values of C, the shape of the paraboloid remains the same for any value of C chosen. Therefore, $C = 1$ has been used for the sake of simplicity. Now, the problem is reduced to finding one of the parameters, given that $b = 1-a$. Thus, a is found by solving an optimization problem where multiple pairs of $(\mu, \lambda_p, \bar{R}_p)$ points that are assumed to, according to author experiences, have roughly the same cost value, are fitted as close as possible to the function (2). The reason why the cost of pairs of points are considered, instead of the cost of single points, is to minimize their difference, voiding the need of guessing/estimating the actual cost value for each of the points which, in fact, is not relevant. Then, by having a set of N pair of points $\mathbf{J} = \left[(J_{1,1}, J_{1,2}), ..., (J_{N,1}, J_{N,2})\right]$, assuming that $J_{i,j} \approx J_{i,j+1},\ \forall i \in \{1, ..., N\}$ (that is, the different points are assumed to have roughly the same cost), the following optimization problem is to be solved.

$$\arg\min_a \sum_{i=1}^{N} \left(J_{i,1} - J_{i,2}\right)^2 \quad (4)$$

In Table I, a set of $N = 5$ pairs of points is listed, with which the optimization problem is solved. The solution of (4) for the set of points in Table I is $a = 0.75757$, and for this value of a the level curves of (2) are represented in Figure 1, where the pairs of points used to fit the parameters a and b have also been depicted. The set of pairs in Table I, except for pair $i = 3$, are meant to force the cost function J_p to have almost vertical or horizontal level curves in certain regions of the domain. When a local region contains vertical curves, according to the axes in Figure 1, changes in the parameter $\bar{R}_p$ result only in insignificant change to the cost value. Similarly, local regions where the level curves are horizontal lines are regions where λ_p become almost irrelevant, since changes in this parameter will not affect the value of the cost J_p. With this methodology, it is possible

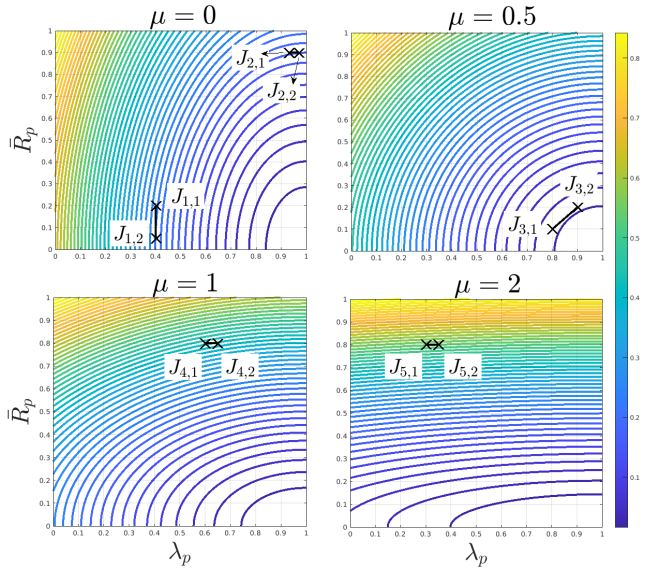

Fig. 1: Level curves of cost function J_p in (2), with $a = 0.75757$ and $b = 1 - a$, fitted using the pairs of points in Tab. I.

to tune the cost function more accurately by determining at which urgency levels the cost function should become more (or less) sensitive to certain values of each of the parameters. In the special case of pair $i = 3$, the pair of points are chosen to achieve an even contribution of both parameters around $\mu = 0.5$, meaning that the cost should be equally sensitive to both, λ_p and $\bar{R}_p$ around this level of urgency (see the middle plot in Figure 2).

The yellow zones in Figure 1 represent high cost regions, namely, undesired landing locations. The blue zones, by contrast, represent low cost regions, being the better locations to land. Note, thus, how the yellow and blue regions are flowing, continuously moving the high cost regions from the left side to the upper side with the increase of the urgency level μ. This change is motivated by the fact that for low μ levels the drone should be able to travel further with relative low risk, aiming for higher confidence landing spots. However, the drone should land as soon as possible if the urgency increases, due to the high probability of imminent loss of control. Hence, the decision function will always aim for the closest landing spots detected if the urgency is high, in expense of a possible deteriorated confidence level of the landing spot. Besides, in spite of the possibility that by taking the closest location the confidence level of the landing spot, λ, becomes extremely deteriorated, it is still safer (to some extent) to attempt a landing (or crash-landing) procedure there rather than some other landing point that has not even been detected and processed by the aircraft, which could potentially happen if the aircraft losses control in an attempt to reach further landing spots.

B. Sensitivity of the Decision Function

An easy way of identifying the contribution of the parameters to the cost is by inspecting the partial derivatives of the function, which will provide a measure of the sensitivity of J_p with respect to each of the parameters. However, only the partial derivatives with respect to λ and $\bar{R}$ are taken in this case, which will be evaluated for increasing values of μ to see how the sensitivity of J_p changes with the urgency level. In the same manner, the derivatives will be evaluated in three different values of α to emphasize the effect of this tuning coefficient. Recall that high values of α simulate a more robust drone.

The partial derivatives are

$$\frac{\partial J}{\partial \lambda} = 2\alpha w_1(\mu)\frac{(1-\lambda_p)}{a}\,, \tag{5a}$$

$$\frac{\partial J}{\partial \bar{R}} = 2(1-\alpha) w_2(\mu)\frac{\bar{R}_p}{b}\,. \tag{5b}$$

Given that (2) is quadratic with respect to λ and $\bar{R}$, it is obvious that its partial derivatives are curves with a slope dependent on μ and α. Since a and b were found for the standard case $\alpha = 0.5$, which represent an aircraft with average technical characteristics, the sensitivity of the cost will also be shown for $\alpha = 0.2$ and $\alpha = 0.8$ in order to examine how the penalizations are modified for aircraft that are less or more reliable and robust, respectively.

In Figure 2 the partial derivatives in (5) are evaluated for $\mu \in [0, 2]$ (see first axis) to visualize the change due to for increasing urgency level, and also for three arbitrary drones with coefficients $\alpha = \{0.2, 0.5, 0.8\}$, plots from left to right. The contribution, or relevance, of each parameters with respect to the cost is related to the slopes in (5) given the linearity of the partial derivatives.

Notice that the partial derivative associated to λ has negative gradient, whereas the partial derivative associated to $\bar{R}$ has positive gradient, for any value of μ and α. Negative gradients mean that low values of that parameter at hand are more penalized, and the other way around for positive gradients. If the gradient is 0, or close to, it means that the parameter has roughly no contribution to the cost. In this interpretation, it does not matter whether the gradient is negative or positive, because our interest is in the absolute contribution of the parameter. Therefore, the absolute value of the gradients are plotted in Figure 2. This makes it easier to compare the relevancy of both parameters to the cost function. Note that the middle plot in Figure 2, corresponding to $\alpha = 0.5$, has a mark at $\mu = 0.5$. At this point, the absolute values of the slopes for both partial derivatives are almost equal. When solving the optimization problem as shown in Figure 1, this was indeed intended to happen by finding a solution where, among other characteristics, the contribution of both parameters λ and $\bar{R}$ were approximately equal for $\mu = \alpha = 0.5$.

Inspecting Figure 2 becomes easier now, and multiple things can be noticed. Firstly, independently of α, the relevance of λ in the cost tends to zero as μ increases. Secondly, $\bar{R}$ contributes more as the urgency level increases. This makes reference to the situation described previously, where an increase in urgency makes landing sooner more important, leading to prioritizing the closest landing spots

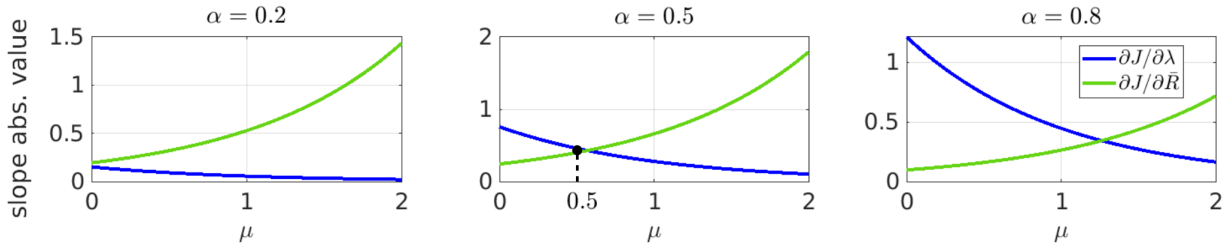

Fig. 2: Sensitivity of J_p with respect to λ_p (blue) and $\bar{R}_p$ (green), based on the partial derivatives (5). The partial derivatives are evaluated for increasing values of $\mu \in [0, 2]$ (see x-axis), representing an increase on the urgency to land, and for three different values of α (from left to right: $\alpha = 0.2, 0.5, 0.8$), simulating three kind of drones with different robust characteristics. The slope value of the partial derivatives (see y-axis) represents the maximum contribution that each parameter can offer to the cost function for every urgency level.

with less concern for the probability measure (or confidence) of the landing spot. Thirdly, if α increases, the parameter λ gains relevance over $\bar{R}$. This still means that, when the urgency level increases, the relevance of λ in the cost decays (exponentially according to $w_1(\mu)$). However, it decays with a certain delay with respect to lower values of α, which allow drones associated to higher α values to pick slightly further landing spots, given that the confidence level λ still plays a role in the decision.

III. TESTS AND RESULTS

A. The role of α

To illustrate the differences between choosing various values of the tuning parameter α, a test is conducted with 11 (λ_p,$\bar{R}_p$) points, placed uniformly along one of the diagonals of the $\lambda - \bar{R}$ domain as shown in the left plot of Figure 3. These points are located from the best λ and worst $\bar{R}$ possible (point 1), to the worst λ and best $\bar{R}$ possible (point 11), by changing their values equally so that the points form a straight line. On the right plot of Figure 3 it is shown the landing location selected, among the previous 11 points, by three different functions J_p, each with a different α value and for every urgency level μ up until all decisions function have chosen the last point.

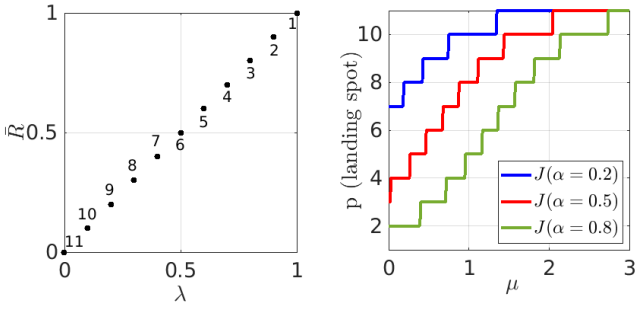

Fig. 3: Eleven $(\lambda_p, \bar{R}_p)$ points are uniformly placed along one of the diagonals of the domain (left). They are all evaluated in J_p through $\mu \in [0, 3]$, for $\alpha = \{0.2, 0.5, 0.8\}$. The point showing the minimum cost value is plotted for each α (right).

This shows how for low urgency values the decision functions prioritize λ over $\bar{R}$. With the increase of urgency level, $\bar{R}$ becomes more relevant than λ and, therefore, closer locations are selected. It can also be seen as α allowing the curves to shift towards the sides, so that further and better spots can be reached. Note that when the decision cost is jumping between the middle points, it does it faster than when getting closer to the points in the corners due to the elliptic shape of the cost function and the weights w_1 and w_2.

Finally, to see the effect of α in action, a simulation is performed where a set of (λ_p,$\bar{R}_p$) points are drawn from a uniform distribution, each of these points representing a landing location detected and processed by *Find* for suitability. The position of the points are shown in Figure 4. These points are evaluated on the cost function J_p for $\mu = 0$ (low urgency) and $\mu = 1$ (high urgency) and compared for the values $\alpha = \{0.2, 0.5, 0.8\}$. The selected landing spot (lowest cost) is marked with a red circle. The level curves of J_p are also shown in the figures. With the decision taken for $\mu = 0$ as reference, it is worth noticing how the jump to closer landing locations for $\mu = 1$ is larger the smaller the value of α is, while the initial decision is maintained for $\alpha = 0.8$.

B. The role of μ

A final general test has been conducted for $\alpha = 0.5$, where the same procedure of drawing random points has been used. This time, five random sets of random (λ_p,$\bar{R}_p$) points have been drawn, representing five different cases where the algorithm should take the decision of where to land. For each case, 4 different urgency levels $\mu = \{0, 0.5, 1, 2\}$ are studied presenting a total of 20 different scenarios as shown in Figure 5. Yet again, each of the points are evaluated in the cost J_p for the respective value of μ, and the point providing the minimum cost is circled in red ○, denoting the selected landing location.

IV. CONCLUSION

This work proposes a relatively simple method for determining an appropriate landing location for a malfunctioning unmanned aircraft. The method uses only three input parameters that can be generated either by the autopilot or by an

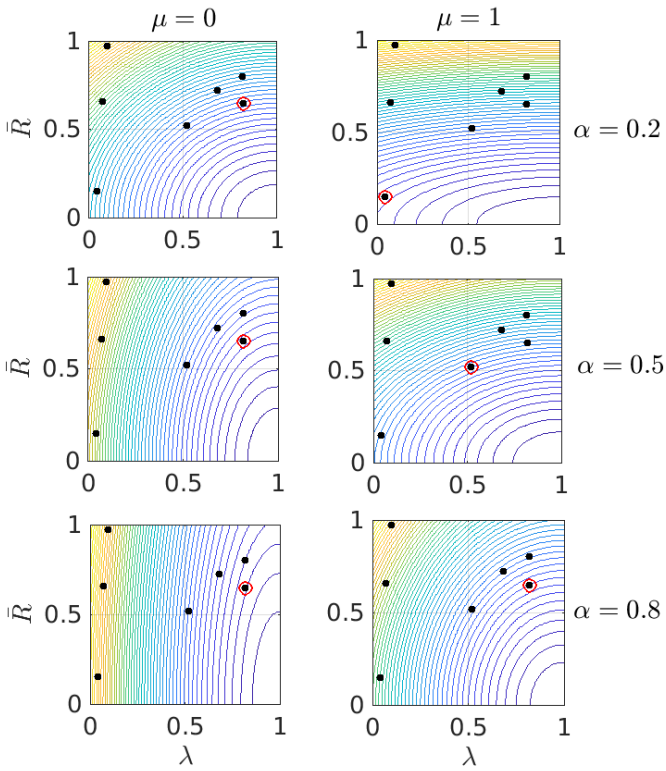

Fig. 4: Seven random $(\lambda_p, \bar{R}_p)$ points sampled from a uniform distribution are evaluated in the decision function J_p for three different drone cases, i.e. $\alpha = \{0.2, 0.5, 0.8\}$, and for two urgency scenarios, i.e. $\mu = \{0, 1\}$. The point with minimum cost value is circled in red ○, denoting the location selected to perform the landing procedure. The level curves of J_p are also superposed in the plots.

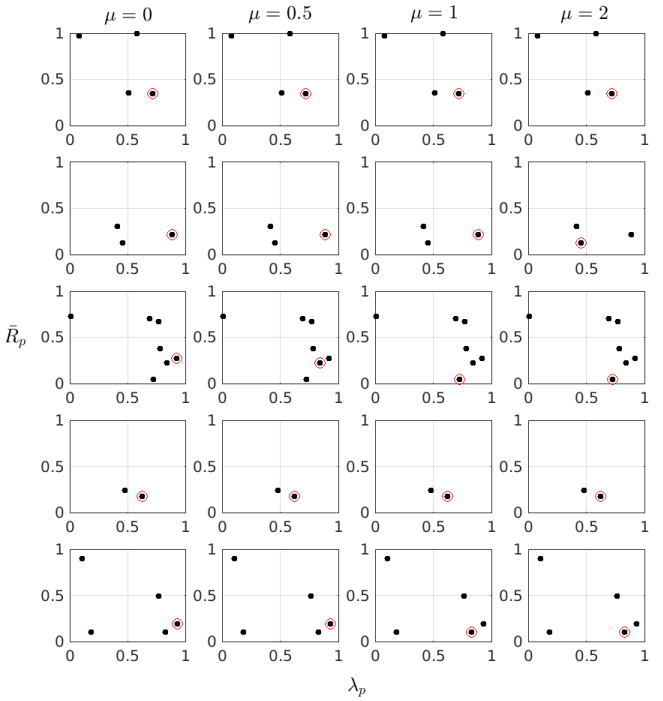

Fig. 5: Random $(\lambda_p, \bar{R}_p)$ points that simulate sets of landing locations detected are evaluated into the cost function J_p for $a = 0.75757$, $b = 1 - a$ and $\alpha = 0.5$. Each set of random points drawn are evaluated for 4 different urgency levels $\mu = \{0, 0.5, 1, 2\}$, as represented in each column, and the selected point according to the value of J_p is circled in red ○.

additional device (such as SafeEYE). The development of the method is based on considerations of how a human would prioritize a landing (in a sense a feed forward approach) rather than existing data on failed and successful landings of error-stricken aircraft (in a sense a feedback approach). This is mainly because there is no existing data set available to train a decision function through a neural network or similar, and the scope of the SafeEYE project does not envision the creation of such data set.

The method proposed, based on a cost function, takes a decision according to three parameters; the urgency level (μ), and the probability measure and distance to the landing spot (λ and $\bar{R}$). In addition, the solution can be tune-able by the action of a single parameter (α), depending on the robustness of the type of drone at hand.

Notice that the selection of the landing location is based solely in 3 parameters, plus the tune-able parameter α. These are considered the most essential in order to solve the decision problem, however, there is a lot of room to improve and refine the method by including other parameters into the cost function, such as wind, aircraft's velocity, clusters of landing locations, etc. The proper methodology to determine the value of the parameters μ, λ and α is left as future work. However, a methodology on how to detect landing locations and compute its associated probability λ is proposed in [7].

ACKNOWLEDGEMENT

This work is supported by the SafeEYE project grant no. 7049-00001 from Innovation Foundation Denmark

REFERENCES

[1] A. Kushleyev, B. MacAllister and M. Likhachev, "Planning for landing site selection in the aerial supply delivery," 2011 IEEE/RSJ International Conference on Intelligent Robots and Systems, San Francisco, CA, 2011, pp. 1146-1153.

[2] Thiels, Cornelius & Aho, Johnathon & Zietlow, Scott & Jenkins, Donald. (2015). Use of Unmanned Aerial Vehicles for Medical Product Transport. Air Medical Journal. 34. 10.1016/j.amj.2014.10.011.

[3] Tvaryanas, Major A & Thompson, William & Constable, Stephen, "The U.S. Military Unmanned Aerial Vehicle (UAV) Experience: Evidence-Based Human Systems Integration Lessons Learned," In Strategies to Maintain Combat Readiness during Extended Deployments – A Human Systems Approach (pp. 5-1 – 5-24). Meeting Proceedings RTO-MP-HFM-124, Paper 5

[4] Desaraju, Vishnu & Michael, Nathan & Humenberger, Martin & Brockers, Roland & Weiss, Stephan & Nash, Jeremy & Matthies, Larry. (2015). Vision-based landing site evaluation and informed optimal trajectory generation toward autonomous rooftop landing. Autonomous Robots. 39. 10.1007/s10514-015-9456-x.

[5] Reimann, S. & Amos, J. & Bergquist, E. & Cole, J. & Phillips, J.& Shuster,S.: UAV for reliability technical report december AEM 4331aerospace vehicle design (2013)

[6] La Cour-Harbo, A. (2019). Quantifying Risk of Ground Impact Fatalities for Small Unmanned Aircraft. Journal ofIntelligent and Robotic Systems, 93(1-2), 367-384. https://doi.org/10.1007/s10846-018-0853-1

[7] Bektash, O. M. & Pedersen, J. N. & Gomez, A. R. & la Cour-Harbo, A. (Accepteret/In press). Automated Emergency Landing System for Drones: SafeEYE Project. I Proceedings of the International Conference for Unmanned Aircraft Systems 2020 International Conference on Unmanned Aircraft Systems (ICUAS)

[8] A. Johnson, J. Montgomery, & L. Matthies. Vision guided landing of an autonomous helicopter in hazardous terrain. In Proc. of the IEEE Intl. Conf. on Robot. and Autom., pages 3966–3971, 2005.

[9] Pingyuan Cui, Dantong & Ge, Ai Gao. Optimal landing site selection based on safety index during planetary descent. Acta Astronautica. Volume 132, Pages 326-336, ISSN 0094-5765, 2017.

[10] Ayhan, Bulent & Kwan, Chiman & Um, Yool-Bin & Budavari, Bence & Larkin, Jude. (2018). Semi-Automated Emergency Landing Site Selection Approach for UAVs. IEEE Transactions on Aerospace and Electronic Systems. PP. 1-1. 10.1109/TAES.2018.2879529.

[11] Guo, Xufeng & Denman, Simon & Fookes, Clinton & Mejias, Luis & Sridharan, Sridha. (2015). Automatic UAV Forced Landing Site Detection Using Machine Learning. 2014 International Conference on Digital Image Computing: Techniques and Applications, DICTA 2014. 10.1109/DICTA.2014.7008097.

[12] Muhammad Faheem, Rao & Aziz, Sumair & Khalid, Adnan & Bashir, Mudassar & Yasin, Amanullah. (2015). UAV Emergency Landing Site Selection System using Machine Vision- Journal of Machine Intelligence. Journal of Machine Intelligence. 1. 13-20. 10.21174/jomi.v1i1.24.

[13] Hult, Robert & Reza Sadeghitabar. “Path planning for highly automated vehicles.” (2013).

[14] La Cour-Harbo, A. (Accepted/In press). Ground impact probability distribution for small unmanned aircraft in ballistic descent. In Proceedings of International Conference on Unmanned Aircraft Systems 2020 International Conference on Unmanned Aircraft Systems (ICUAS)